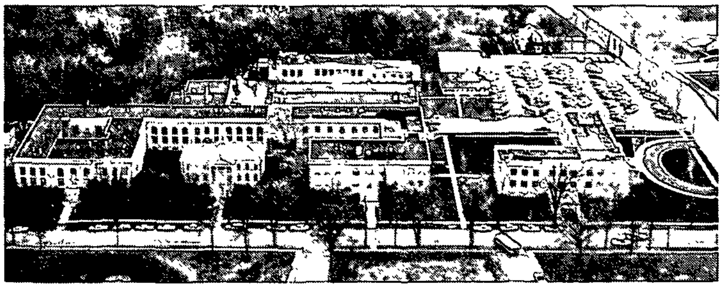

THE INSTITUTE OF PAPER CHEMISTRY, APPLETON, WISCONSIN

IPC TECHNICAL PAPER SERIES

NUMBER 241

CORROSION FATIGUE TESTING OF SUCTION ROLL ALLOYS

RONALD A. YESKE

JUNE, 1987

Corrosion Fatigue Testing of Suction Roll Alloys

Ronald A. Yeske

This manuscript is based on results obtained in IPC Project 3309, and is to be presented at the TAPPI Engineering Conference in September, 1987 in New Orleans

CORROSION FATIGUE TESTING OF SUCTION ROLL ALLOYS

Ronald A. Yeske, Section Leader
Corrosion and Materials Engineering
The Institute of Paper Chemistry
P.O. Box 1039 Appleton, WI 54912

ABSTRACT

Crack growth rate measurements have been used to examine the resistance of various suction roll alloys to fatigue crack growth in the near-threshold regime where the crack advance per stress cycle is very small. The effects of exposure to various simulated paper machine whitewaters during crack growth have been determined. The deleterious effects of imposition of a tensile mean stress during crack growth have also been determined and related to residual stress effects associated with heat treatment of commercial rolls. The threshold stress intensity for crack growth is interpreted in terms of the critical flaw size for crack growth under nominal service loading conditions.

INTRODUCTION

Cracking of suction rolls in service has been a chronic and costly problem for the paper industry in recent years. The extent of the problem has been documented for Canadian mills by Garner (1) and for mills in the United States by Moskal et al. (2). Both studies report frequent failures of suction rolls of all types, although bronze and martensitic stainless steel suction rolls in press positions appear to be the most vulnerable. Garner reported that approximately ninety rolls had failed in a nine year period in Canadian mills. The new duplex stainless steel suction rolls appear to be much more resistant than either the bronze or the martensitic stainless steels such as CA-15, but failures of several of these duplex stainless steels have also been reported.

The failure of suction rolls apparently occurs by the initiation and growth of fatigue cracks. Fatigue failure is implicated in suction roll cracking because of the cyclic nature of the loading imposed on suction rolls, and because of the absence of clear evidence of other forms of cracking. Stress corrosion cracking has also been implicated as an alternative form of cracking, but only in a few cases where heat treatment of the rolls produced a metallurgical structure which was susceptible to this form of cracking.

There have been relatively few instances where suction roll failures have been carefully documented in the published literature (3). Most of the available information on suction roll cracking has been made available at meetings of the TAPPI subcommittee on suction rolls by vendors or owners of suction rolls that have failed in service.

In general, two types of fatigue failure have been encountered. For alloys with marginal resistance to erosion-corrosion, such as 85Cu-5Pb-5Zn-5Sn bronze, failure often occurs after erosion-corrosion has enlarged the holes in the suction roll as shown in Fig. 1. This enlargement reduces the load-bearing ligament between adjacent holes, raising the cyclic stress level until fatigue failure ensues. For materials with greater resistance to erosion-corrosion, such as the duplex stainless steels, crack initiation and growth often occur without any visible evidence of corrosion (Fig. 2).

Fig. 1. Hole enlargement in a bronze suction roll which led to fatigue failure.

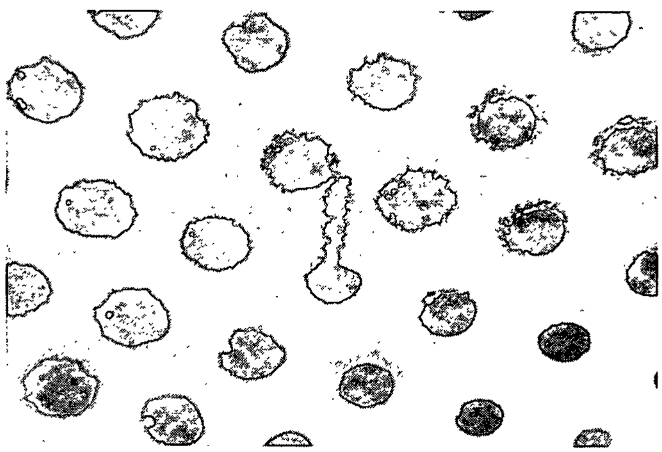

Fig. 2. A fatigue crack propagating from a hole in a duplex stainless steel suction press roll.

The characteristics of failure vary from roll to roll, but circumferential cracking in the middle region of the roll predominates. Cracking may begin at the inside or outside surface of the roll shell, but cracking at the inside surface is apparently more common. Nearly all cracking is confined to the middle two-thirds of the shell, corresponding to the location of the largest bending moments and highest cyclic stresses.

There have been no published reports of careful attempts to correlate suction roll failure with details of suction roll metallurgy/fabrication or paper machine whitewater characteristics. Tensile residual stresses introduced into suction rolls have been implicated in premature failure of duplex stainless steels which were water-quenched before installation, but the evidence for this involvement

1

of tensile residual stresses is not unequivocal. Higher nip loading and increased length of rolls have also been implicated as being partially responsible for the accelerated pace of suction roll failures.

Suction roll lifetimes may conveniently be divided into initiation and propagation periods which are separated in time by the emergence of a visible crack. On smooth surfaces, fatigue crack initiation occurs by irreversible deformation processes that occur in the metal as a result of cyclic loading. Irreversible deformation leads to the initiation of a crack which then propagates under the influence of fluctuating loads. When discontinuities are present on the surface of metal components subjected to cyclic loading, the number of cycles required for crack initiation is reduced and the fraction of lifetime spent in propagation is correspondingly higher. A similar situation obtains when the failure occurs on surfaces wetted by a corrosive medium such as paper machine whitewater. Pits and other surface defects can occur as a result of corrosion, thereby accelerating the onset of cracking. Pits can also retain electrolytes which are far more corrosive than the bulk environments, thereby causing accelerated initiation of cracks. The relative proportions of time spent in crack initiation and growth have not been carefully documented, but several instances are known where suction rolls spent a significant portion of their lifetime in the crack propagation mode.

Although crack propagation is clearly an important segment of suction roll failure, most investigations of fatigue failure of suction rolls have focused on the crack initiation behavior. Resistance of a suction roll alloy to fatigue failure is generally presented in the form of an S-N curve. The S-N curve shows the relationship between the amplitude of the cyclic stress applied to test specimens (S) and the number of times this stress can be imposed before failure occurs (N). If the test specimen is smooth, rather than notched, and the test is conducted in a relatively benign environment, most of the cyclic lifetime is spent in crack initiation and relatively little is spent in crack growth. This is particularly true if the lifetimes are long -- i.e., more than a million cycles. Thus, for long lifetimes, most of the cycles accumulated before failure are spent in crack initiation, and S-N curves are dominated by crack initiation resistance of the material under test.

The correlation between S-N data for various suction roll alloys and the performance of these alloys in service has not been very good. In some published S-N data, alloys with very poor service performance can withstand larger cyclic stress amplitudes in the 100 million cycle regime than alloys which have performed well in service (4).

Only a few studies have focused on the resistance of suction roll alloys to propagation of fatigue cracks (4-7). In these studies, interest has focused on the characteristics of crack growth in the near-threshold regime where the rate of crack propagation is very low -- on the order of 10^{-10} m/cycle. Higher rates of crack growth can be measured, of course, but the behavior in this regime does not represent a significant fraction of the lifetime of actual suction rolls. For example, at crack growth rates of 10^{-7} m/cycle, a suction roll which rotates at 500 rpm will experience a meter of crack growth in about two weeks. Interest has also focused on the thresholds below which crack growth will not occur, as described below.

The objective of this study was to characterize the crack growth rate behavior of several different suction roll alloys in the growth regime where cracking is very slow and on the verge of cessation. The relative resistance of several alloys was compared by conducting standardized crack growth tests in various simulated paper machine whitewaters.

Crack Propagation Concepts

It has been known for many years (8) that the rate of crack growth during fatigue loading depends on other parameters besides the magnitude of the cyclic forces imposed on the cracked material. In general, it has been shown that the driving force for crack growth depends on the instantaneous length of the crack and the geometry of the cracked material, in addition to the magnitude of the cyclic loading. These three factors are combined in a quantity called the cyclic stress intensity range, ΔK.

The expression for the cyclic stress intensity range depends on the size and shape of the cracked structure and the length of the crack in relation to the overall structure. In general, the ΔK expression is a product of three terms -- one each for the cyclic loading, the crack length, and the geometry of the cracked structure. For example, if the cracked structure is an infinitely large sheet containing a crack of length 2a which is perpendicular to the plane of loading as shown in Fig. 3, and the range of the applied stress is σ, the expression for the cyclic stress intensity range is

$$\Delta K = \sigma\sqrt{a}\,\sqrt{\pi} \qquad (1)$$

The dimensional units for the cyclic stress intensity range are $MN \cdot m^{-3/2}$.

If the sheet in the example was of finite width, W, the expression for the cyclic stress intensity range would contain a function of (a/W) to account for the different geometry, as follows

$$\Delta K = \sigma\,\sqrt{a}\ \mathrm{fn}(a/W) \qquad (2)$$

The stress intensity factors for a large number of geometries and loading conditions have been determined and summarized in compendia (9).

Since the cyclic stress intensity denotes the driving force for crack growth, it can be used to compare crack growth data obtained from tests using a variety of crack lengths and test specimen geometries. For example, we might expect that the rate of crack growth at a given ΔK would be the same, regardless of whether the data were obtained from a specimen with a short crack and high cyclic loads, or a long crack experiencing lower stresses. The concept is also useful for predicting the rate of crack growth in service, provided the loading

2

conditions can be determined and the stress intensity formula for the cracked structure can be calculated.

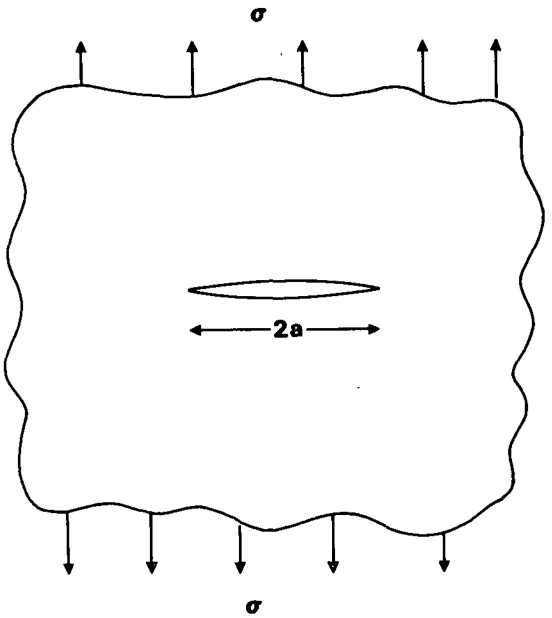

Fig. 3. Schematic representation of a cracked panel corresponding to the stress intensity expression given in Eq. (1).

In practice, fatigue crack growth rate data are obtained using one or two convenient test specimens whose stress intensity formulae are well known. Most tests are conducted with the compact tension specimen shown in Fig. 4, whose stress intensity formula is tabulated in ASTM Standard E647 as a function of the size of the specimen, the crack length, and the cyclic forces applied to the specimen through pin grips.

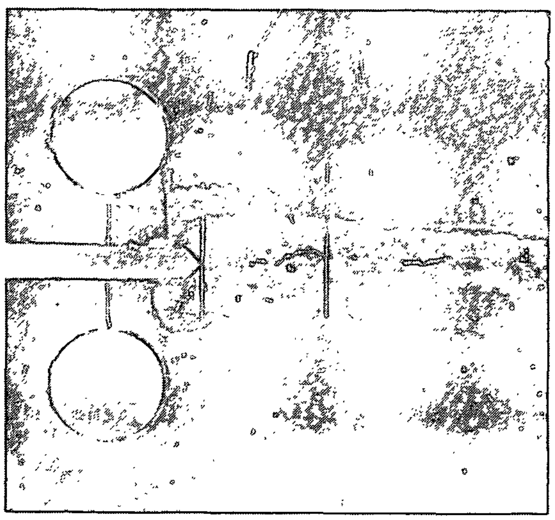

Fig. 4. Photograph of a compact tension test specimen after failure.

In a typical test to determine the crack growth rates as a function of ΔK, a compact tension specimen is loaded in pulsating tension until a fatigue crack begins to propagate from the machined notch. Once the crack begins to grow, the length of the crack is determined periodically, usually with a travelling microscope equipped with a vernier stage, until the specimen fails. If the amplitude of the cyclic loading is constant, the stress intensity range continues to increase throughout the test, since the crack length term in the stress intensity formula increases as the crack grows. The average rate of crack growth (per load cycle) is inferred from the change in crack length and the number of intervening stress cycles. A single test specimen can be used to obtain growth rate data over a range of ΔK values, but several specimens are usually required to characterize the entire spectrum of crack growth behavior. Since the rate of growth often varies by several orders of magnitude, the growth rate data are usually presented on a log-log plot of growth rate <u>vs</u>. cyclic stress intensity range, as shown in Fig. 5.

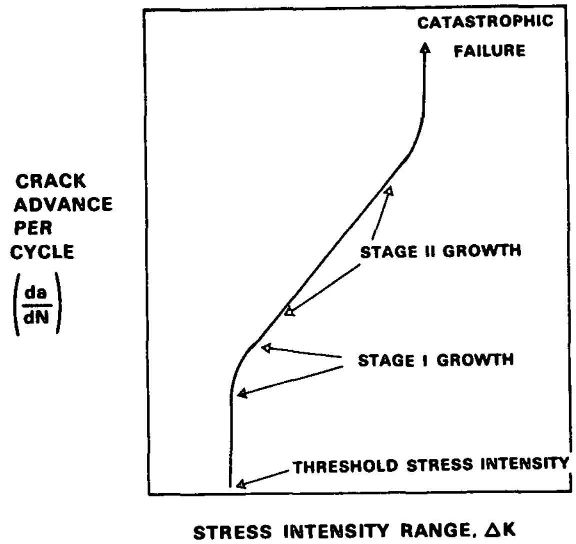

Fig. 5. Schematic diagram of log-log plot of crack growth data.

Three stages are often evident in the growth rate plot. When the cyclic stress intensity is very high (Stage III), the specimen is on the verge of failure by simple overload and the growth rates are high. In Stage II, stable crack growth occurs over a wide range of ΔK values and a power law relationship between the growth rate and the stress intensity range is often revealed as a linear segment on the log-log plot. Stage I is marked by low growth rates and a strong dependence of growth rate on ΔK. In most cases, a threshold stress intensity, ΔK_{th}, exists below which crack growth ceases. As described above, the near-threshold regime in Stage I is the only regime of interest for suction roll applications.

Accurate determination of the threshold stress intensity for crack growth must be done with great

3

care, because of the opportunities for production of artifacts through inadvertent errors in the test procedure. For example, unconservative threshold stress intensities are usually obtained if the tests are conducted by gradually increasing the stress intensity imposed on a test specimen and noting the stress intensity corresponding to the onset of crack growth. The acuity of the crack tip is of great importance in threshold determination, and the blunt notches that are machined into test specimens generally require higher stress intensities to get cracks started. The most reliable threshold data are obtained by a technique called load-shedding, wherein the load applied to a sharp crack is gradually reduced until the crack ceases propagating. Because of the possibility of introducing compressive residual stresses in the zone ahead of the crack tip, the load shedding must be completed in very small decrements and with intervening periods of growth at the reduced stress intensity.

Theoretically, the threshold stress intensity can be used to estimate the loading that a structure can experience without propagation from a pre-existing flaw of known dimensions. For example, if the threshold stress intensity for a given material is known to be 5 $MN \cdot m^{-3/2}$, and a pre-existing flaw of 1 mm (0.001 m) is assumed, Eq. (1) can be used to determine the maximum stress that can be imposed on an infinite sheet without crack growth -- 90 MN/m^2, in this instance. Alternatively, if the loading conditions are known, the critical flaw size that will allow crack growth to commence can be estimated. This critical pre-existing flaw size can then be compared with the size of flaws known to exist in the structure, or with the size of flaws which can easily be discovered using nondestructive testing methods.

Although fatigue crack growth can be made to occur in innocuous environments -- including vacuum -- the presence of corrosive environments can have a dramatic effect on the crack growth behavior. Exposure to aggressive environments generally reduces the threshold stress intensity for crack growth and shifts the entire crack growth rate curve upward and to the left, often increasing growth rates in Stage II by an order of magnitude or more.

In general, the material with the highest threshold stress intensity and the lowest rate of growth in Stage I will be the most resistant to crack growth in circumstances where large numbers of stress cycles are imposed on the structure. Behavior in Stages II and III, while interesting, will not have a significant effect on the fatigue lifetime. Indeed, if the cyclic stress intensity in service straddles the threshold stress intensities for two materials, the material with the lower threshold will inevitably crack, while the material with the higher threshold will remain inviolate.

EXPERIMENTAL PROCEDURES

Crack growth rate tests were conducted by exposing compact tension specimens to fatigue loading while they were immersed in one of several simulated whitewaters. Average crack growth rates were calculated using periodic measurements of the crack length. Threshold stress intensities for crack growth were determined by a careful load-shedding regimen. In general, the provisions of ASTM Standard Method E647 (10) were followed, but modified as necessary for threshold determination. The details of the test method have been summarized in a previous publication (4).

Five commercial suction roll alloys were tested in this program, including four centrifugally cast roll alloys and one wrought alloy. The materials and their nominal compositions are given in Table 1. Each alloy has been used in commercial rolls with varying degrees of success. Alloys 75 and VK-A378 appear to have an unblemished record in suction roll applications, while Alloys 63 and VK-A171 have experienced numerous failures. The service behavior of the wrought 3RE60 alloy is more difficult to assess. Rolls made with this alloy apparently experienced some early failures, but modification of the heat treating procedure apparently stopped subsequent failures. All materials were provided by the vendors in the form of rings or blocks with the appropriate heat treatment for suction roll application.

Table 1 Suction roll alloys in the test program

Alloy	Cr	Ni	Mo	Cu	C	Fe	History
Alloy 75	26	6.8	--	--	0.03	Bal	Uncracked
VKA378	20	5	2	4.5	0.06	Bal	Uncracked
3RE60	18.5	4.7	2.8	--	0.03	Bal	Some cracking
VKA171	23	8.3	1.2	--	0.06	Bal	Some cracking
Alloy 63	22.5	8.5	1.7	--	0.05	Bal	Severe cracking

Compact tension specimens with a thickness of approximately 12 mm were machined from the suction roll segments such that the plane and direction of crack growth mimicked the predominant mode of failure in service.

The test specimens were subjected to pulsating tension loading with a sinusoidal waveform and a frequency of 25 Hz. Although suction rolls clearly experience tension-compression loading during service, it is generally accepted that compressive loading has little effect on crack growth behavior but introduces a significant increase in complexity of the test method. Tests were conducted with one of three mean stress conditions corresponding to an R-ratio of 0.04, 0.1, or 0.5, where

$$R = \frac{K_{min}}{K_{max}} \qquad (3)$$

and K_{max} and K_{min} are the maximum and minimum stress intensities applied to the specimen during one stress cycle. An R value of 0.04 corresponds to loading with a low mean stress, whereas R equal to 0.5 represents a significant tensile mean stress condition.

Tests were conducted either in air or in one of several simulated paper machine whitewaters listed

4

in Table 2. To date, tests have been conducted in eight different simulated whitewaters containing sodium salts of chloride, thiosulfate, and sulfate anions. Environments B and C are TAPPI whitewaters I and II, respectively, recommended for use in Ref. (11). Several low pH environments were employed in order to simulate the acidic conditions that develop in pits and beneath deposits on high chromium alloys. All tests in simulated whitewaters were conducted at a temperature of 50 C, while tests in air were conducted at ambient temperature. Provisions were made to insulate the specimens during testing to avoid artifacts associated with inadvertent galvanic contact between the test specimen and other metals.

Table 2 Simulated white waters

ENVT	Cl^- ppm	SO_4^{--} ppm	$S_2O_3^{--}$ ppm	pH
A	1000	0	0	4.7
B*	100	1000	0	3.5
C**	1000	1000	0	3.5
D	200	500	50	4.0
E	1000	0	0	3.5
F	200	500	10	4.0
G	1000	0	0	1.0
H	200	500	50	1.0

*TAPPI 1.
**TAPPI 2.

RESULTS

General Crack Growth Behavior

All of the materials examined in this study showed classical fatigue crack growth behavior, with obvious Stage I and Stage II growth, and clear threshold stress intensities. Growth rates as low as 1.5 10^{-10} m/cycle were measured. No macroscopic crack branching was observed, although considerable microscopic crack branching was evident in the crack path of cast alloy specimens. The crack path in the wrought specimen was straight and unbranched -- even on a microscopic scale -- compared to the cast alloys. Reproducibility of the crack growth rate data had been documented in a previous report (4).

The corrosion resistance of most of the test alloys was very good in the corrosive whitewater environments. Alloy 75 showed some susceptibility to corrosive attack, particularly in the thiosulfate environments. However, there was no apparent correlation between corrosion susceptibility and resistance to corrosion-assisted fatigue crack growth in these tests.

Crack Growth Behavior in Air

Tests in air revealed moderate differences in the crack growth behavior of the five alloys tested in this investigation. The dependence of crack growth rates on stress intensity range for the five alloys is shown in Fig. 6. These tests were all conducted at an R-ratio of 0.1. The apparent threshold stress intensity range for crack growth ranged from 9 $MN \cdot m^{-3/2}$ for the 3RE60 alloy to approximately 14 $MN \cdot m^{-3/2}$ for Alloy 75. In general, the alloy with the highest threshold also exhibited the lowest rate of growth at any higher stress intensity range.

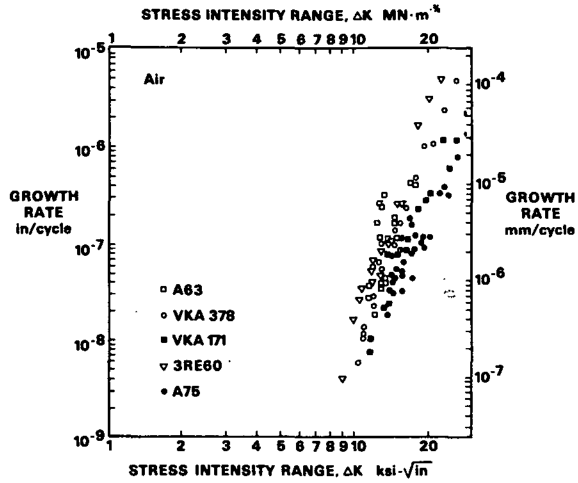

Fig. 6. Crack growth data for five suction roll alloys tested in air at an R-ratio of 0.1.

Environmental Effects on Crack Growth

All of the alloys tested exhibited some reduction in threshold stress intensity range as a result of exposure to the simulated whitewater environments during fatigue testing. The threshold stress intensities for crack growth ranged from 1 to 10 $MN \cdot m^{-3/2}$, depending on the material tested and the corrosiveness of the test environment.

In general, the relative ranking of the resistance of the five alloys remained the same for tests in aggressive environments as it was in air, with Alloy 75 exhibiting the highest threshold, 3RE60 the lowest threshold, and the thresholds for the other alloys falling in between.

The thresholds for crack growth in a dilute chloride environment at a pH of 3 are shown in Fig. 7 for the five alloys tested in this program. These tests were conducted at an R-ratio of 0.1, corresponding to a moderate tensile mean stress. Alloy 75 exhibited the highest threshold stress intensity in this environment -- 10 $MN \cdot m^{-3/2}$ -- compared to a threshold obtained in air of approximately 13 $MN \cdot m^{-3/2}$. The other alloys experienced a similar lowering of thresholds, compared to the values obtained in air.

Further acidification of the dilute chloride environment to a pH of 1 introduced a further reduction in the threshold stress intensities for crack growth, as shown in Fig. 8. Once again, the ranking of the resistance to cracking, as determined by the threshold stress intensities for cracking, remained the same. Alloy 75 exhibited a high threshold for crack growth, whereas 3RE60 exhibited a very low threshold, and other alloys fell in between. The threshold stress intensities for crack growth in this very aggressive environment

5

were roughly half those obtained in Environment E where the pH was only 3.

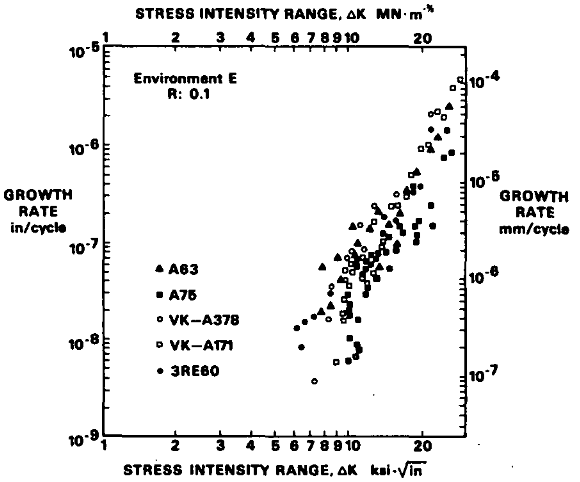

Fig. 7. Crack growth data for five suction roll alloys tested in Environment E containing 1000 ppm Cl^- and a pH of 3. R-ratio = 0.1.

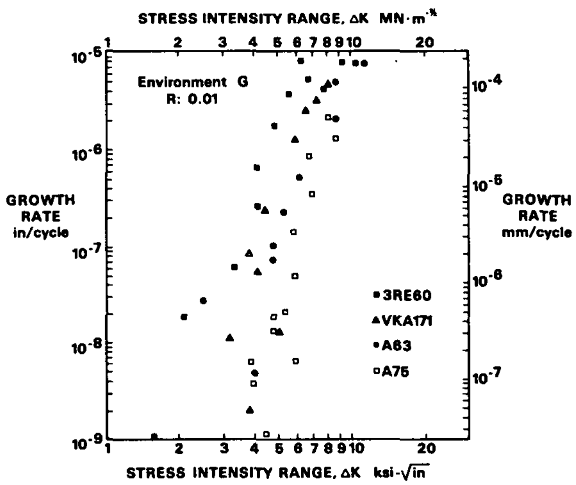

Fig. 8. Crack growth data for four suction roll alloys tested in Environment G containing 1000 ppm Cl^- and a pH of 1. R-ratio = 0.1.

Crack growth data obtained in a more complex test environment containing sulfates, chlorides, and thiosulfates are shown in Fig. 9. Generally speaking, the crack growth behavior for four of the five alloys tested at this pH level was more or less identical to that observed in Environment E at the same pH level. For the fifth alloy, 3RE60, the threshold stress intensity for crack growth fell to only 2 $MN \cdot m^{-3/2}$. Alloy 75 exhibited the highest threshold stress intensity of the five alloys, in spite of considerable corrosion of the specimen during fatigue testing.

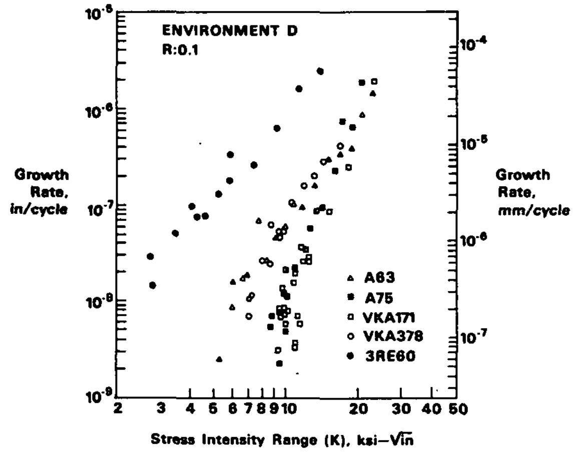

Fig. 9. Crack growth data for five suction roll alloys tested in Environment D containing 50 ppm $S_2O_3^{--}$, 200 ppm Cl^-, and 500 ppm SO_4^{--}. R-ratio = 0.1.

With the exception of the 3RE60, no dramatic effect of thiosulfate additions was observed in tests in Environment D, although the presence of other species prevents an unequivocal comparison of the effectiveness of chlorides and thiosulfates in promoting cracking. Interpretation of the effect of the various anion constituents of the simulated whitewaters must await further tests.

The Effect of pH

The large effect of pH on crack growth characteristics is shown in Fig. 10 for Alloy 63 tested in dilute chloride environments adjusted to three different pH levels. The figure shows the crack growth behavior for tests in 1000 ppm Cl^- environments with the pH adjusted to 5, 3, and 1. The threshold stress intensity for crack growth fell dramatically as the pH was reduced from 5 to 1. A similar effect of lowering pH from 3 to 1 was observed with other alloys in the test program.

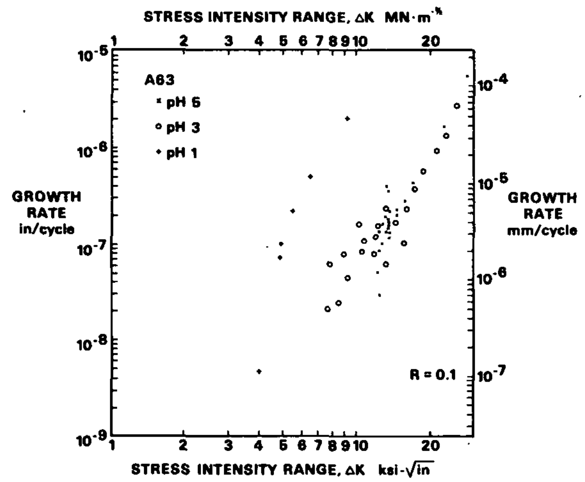

Fig. 10. Crack growth rate data for Alloy 63 tested in a 1000 ppm Cl^- environment at various pH levels.

Effect of Mean Stress

The superimposition of high tensile mean stress during fatigue loading of the test specimens resulted in a significant lowering of the thresholds for crack growth for some of the alloys tested, whereas other alloys were less affected by mean stress. Crack growth rate data for tests in Environment E at an R-ratio of 0.5 are presented in Fig. 11, for comparison with the data shown in Fig. 7 at an R-ratio of 0.1. For Alloy 75, the introduction of a large tensile mean stress reduced the threshold stress intensity for crack growth from 10 to 7 $MN \cdot m^{-3/2}$, as shown in Fig. 12. For VK-A171, on the other hand, imposition of a similar mean stress resulted in a 50% reduction in the threshold stress intensity for crack growth -- from 10 $MN \cdot m^{-3/2}$ to less than 5 $MN \cdot m^{-3/2}$ (Fig. 13).

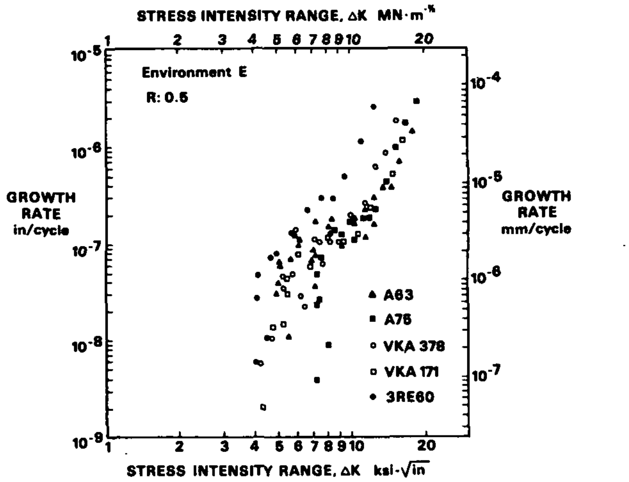

Fig. 11. Crack growth rate data for five suction roll alloys tested in Environment E at an R-ratio of 0.5.

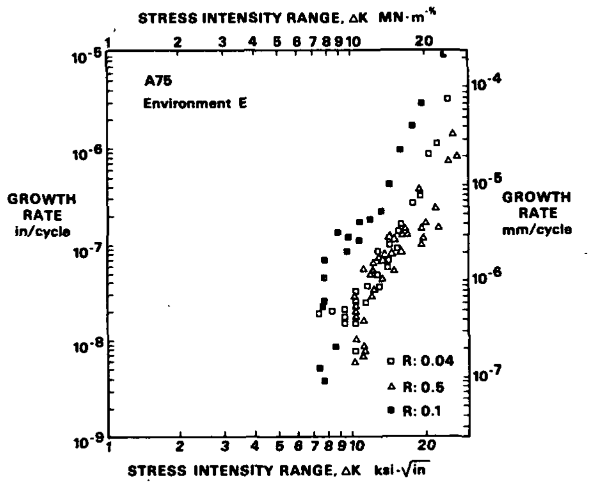

Fig. 12. Data showing the modest effect of mean stress level on crack growth rates in Alloy 75.

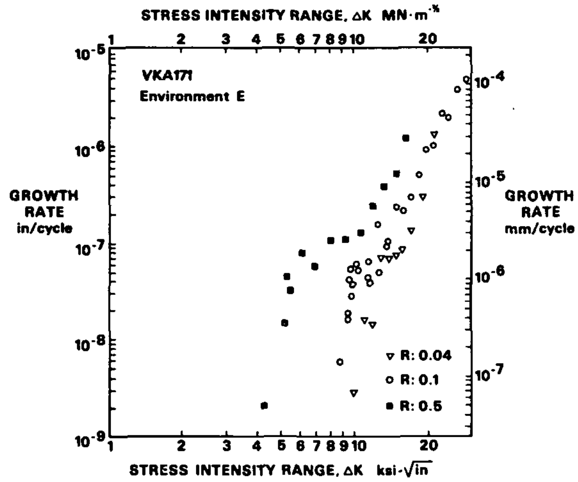

Fig. 13. Data showing a large effect of mean stress on crack growth rates for VK-A171 Alloy.

DISCUSSION

The threshold stress intensities for fatigue crack propagation determined in this study represent a significant difference in resistance to corrosion-assisted cracking. The highest threshold observed in the tests conducted in a simulated whitewater was approximately 13 $MN \cdot m^{-3/2}$ for Alloy 75 tested in a dilute chloride solution at a pH of 3. The lowest threshold stress intensity -- 1.5 $MN \cdot m^{-3/2}$ -- was observed for the 3RE60 alloy tested under high tensile mean stress conditions in Environments D and G. This represents nearly an order of magnitude difference in susceptibility to crack growth in the near threshold regime.

The significance of a tenfold variation in threshold stress intensity can be examined by considering the change in critical flaw size required for crack growth in a hypothetical suction roll. Recall that the critical flaw size corresponds to the smallest defect that can trigger crack growth in a material of known ΔK_{th}, when subjected to fatigue loading of known magnitude. For this comparison, assume that the cyclic stresses are of the order of those cited by Rubenis (12) -- approximately 55 MN/m^2. In the absence of a better formula for the stress intensity of a crack in an actual suction roll, assume the relationship shown in Eq. (1).

At the threshold condition, this relationship becomes

$$\Delta K_{th} = \sigma \sqrt{a_{crit}} \sqrt{\pi}$$

where a_{crit} is the critical flaw size for propagation at a given ΔK_{th}. If ΔK_{th} is 13 $MN \cdot m^{-3/2}$, the critical flaw size is approximately 2 cm. On the other hand, if ΔK_{th} is only 1.5 $MN \cdot m^{-3/2}$, a sharp flaw as small as 0.02 cm is sufficient to allow cracking to proceed.

7

It is instructive to consider these upper and lower limits of the critical flaw size (as derived from the ΔK_{th} values obtained in this study) in light of flaw sizes likely to exist in an actual suction roll. If the suction roll alloy has a ΔK_{th} of 13 $MN \cdot m^{-3/2}$, a sharp flaw approximately 2 cm long will be required for crack propagation to occur under nominal loading conditions. A casting defect 2 cm long will be a rare event, and materials with this high threshold value will generally be resistant to crack growth during routine service. On the other hand, a material with a ΔK_{th} of only 1.5 $MN \cdot m^{-3/2}$ will experience cracking if a sharp flaw longer than 0.02 cm is present. Defects of this size are commonly found in castings, and may also be present in forged or wrought materials as a result of machining marks or other surface damage. A very small flaw will allow a crack to propagate if the threshold stress intensity is low.

Since tensile mean stress and aggressive whitewater conditions have been shown to reduce the value of the threshold stress intensity for crack growth, these conditions are clearly to be avoided in actual suction roll service.

The strong effect of tensile mean stress on crack growth characteristics may explain the susceptibility of some suction rolls to cracking in service. Tensile mean stresses are commonly introduced in metals as a result of heat treatment practices. Some suction rolls, such as A63 and VK-A171, are thought to have high tensile residual stresses as a result of water quenching following heat treatment. The present data suggest that the critical flaw size in these alloys is greatly reduced if large tensile residual stresses are present during fatigue loading. The high residual stresses present in these rolls may reduce the threshold stress intensity, and therefore the critical flaw size, and promote crack growth from very small defects in the material.

The development of acidic conditions under deposits in suction rolls may also explain the susceptibility of suction rolls to corrosion-assisted cracking. Although the highly acidic conditions used in the present testing are unlikely to be found in bulk paper machine whitewaters, highly acidic conditions can develop in pits and beneath crevices as a result of localized corrosion processes. When scales, deposits and biological growths occur on suction rolls, acidification of the liquids trapped beneath these films can occur. The threshold stress intensity data obtained in the present study clearly show that acidification of the environment contacting the roll material results in a significant lowering of the threshold stress intensity. Under these conditions, a corresponding reduction in the critical flaw size for crack growth will occur, perhaps to a point where routine loading will result in crack growth. Maintenance of clean suction rolls would therefore appear to be desirable for prevention of corrosion-assisted fatigue crack growth.

The relative susceptibility of different suction roll alloys may also be explained by the present threshold stress intensity data. In environments where the pH is 3 or above, Alloy 75 maintains a threshold stress intensity for crack growth of 7 $MN \cdot m^{-3/2}$ or higher, whereas the other suction roll alloys generally exhibit lower threshold values. In the critical flaw size analysis presented above, the critical flaw size corresponding to a 7 $MN \cdot m^{-3/2}$ threshold is approximately 5 mm. Casting defects larger than this are relatively rare, and may not appear in the highly stressed regions of the rolls now in service. On the other hand, A63, VK-A171, and 3RE60 consistently exhibit thresholds which are lower than that of Alloy 75, and their cracking in service may occur because the critical flaw size is lower, and perhaps on the order of the defect size in typical suction roll construction. However, the situation with VK-A378, which has a lower threshold than A75 but has not exhibited cracking in service, is not consistent with this interpretation.

CONCLUSIONS

Near-threshold fatigue crack growth rate measurements have shown that the threshold stress intensity for fatigue crack growth is lowered by

* exposure to simulated paper machine whitewaters containing aggressive anions
* acidification of the simulated whitewater environment
* imposition of a tensile mean stress during crack growth.

Differences in critical flaw size for crack growth under nominal cyclic loading conditions may explain the difference in susceptibility of different suction roll alloys to cracking in service applications.

Acknowledgements

Craig Thompson and Mark Revall performed the fatigue testing experiments with unusual skill and dedication, and their contributions to this study are gratefully acknowledged. The provision of suction roll test materials by Beloit Corporation, Sandusky Foundry and Machine Company, Avesta, Valmet, and Kubota is also appreciated.

REFERENCES

1. Garner, A., "Suction Roll Failure in Canada", Proc. 70th Annual Meeting of the Canadian Pulp and Paper Association, Montreal, February, 1984.

2. Wooster, F, Moskal, M., and McNamee, J., Tappi, 62(9): 71(1979).

3. Anliker, D., "Field and Laboratory Examination of Suction Rolls", Proc. TAPPI Engineering Conference, 1984, p. 209.

4. Yeske, R., "Prediction of Suction Roll Performance from Laboratory Testing," Corrosion/86, NACE, Paper No. 147 (1986).

5. Moskovitz, J., and Pelloux, R., "Corrosion Fatigue Behavior of Austenitic-Ferritic Stainless Steels", Corrosion Fatigue Technology, ASTM STP 642, American Society for

8

Testing Materials, Philadelphia (1978) p. 133-145.

6. Bassidi, M., Masounave, J., and Dickson, J., ASM Metals Congress, St. Louis (1982). Available from the American Society for Metals, Metals Park, OH as ASM Technology Series 8201-023.

7. Bassidi, M, Masounave, M., and Dickson, J., Canadian Metallurgical Quarterly 20(3): 317(1981).

8. Broek, D. Elementary Engineering Fracture Mechanics, Martinus Nijhofff Publishers, Boston (1982).

9. Sih, G., Handbook of Stress Intensity Factors, Institute of Fracture and Solid Mechanics, Lehigh University (1973).

10. ASTM Test Method E647, "Constant Load Amplitude Fatigue Crack Growth Rates Above 10^{-8} m/cycle", American Society for Testing Materials, Philadelphia.

11. "Plate Bending Fatigue Testing in a Corrosive Environment", Technical Information Sheet TIS 0402-08, TAPPI, Atlanta (1984).

12. Rubenis, D., "Evaluation of Paper Machine Suction Roll Sheels", Proc. Engineering Conference, Tappi, (1984) p. 579.

9